Effect of Protein Kinase A-Induced Phosphorylation on the Gating Mechanism of the Brain Na^+ Channel: Model Fitting to Whole-Cell Current Traces

Pablo d'Alcantara*, Serge N. Schiffmann,# and Stéphane Swillens*

*Institut de Recherche Interdisciplinaire en Biologie humaine et Nucléaire and #Unité de Recherche sur le Cerveau, Faculté de Médecine, Université libre de Bruxelles, Brussels, Belgium.

ABSTRACT The activity of the voltage-gated Na^+ channel is subjected to modulation through covalent modifications. It has been previously shown that brain Na^+ currents are reduced following the activation of the protein kinase A (PKA) pathway, but the effect of the phosphorylation on the gating mechanism of the channel has not been demonstrated so far. In this study, we analyze the whole-cell Na^+ current recorded in the absence or presence of forskolin, which stimulates the PKA pathway. A minimal molecular model of the gating mechanism of the Na^+ channel is defined to fit the experimental data: it consists of three closed states, one open state, and two inactivated states. We experimentally demonstrate that the kinetics of inactivation from the closed states are not affected by phosphorylation. The results obtained by computer fitting indicate that, among all the kinetic parameters describing the transitions between states, only one parameter is significantly modified in the presence of forskolin, and corresponds to the acceleration of the inactivation from the open state. This conclusion is supported by the analysis of current traces obtained from cells in the presence of a phosphatase inhibitor or loaded with the PKA catalytic unit, and is in agreement with previously reported single channel records.

INTRODUCTION

The modulation of ion channel activity by neurotransmitters and hormones, either through a direct G-protein coupling or through a covalent modification resulting from the production of second messengers and activation of phosphorylation pathways, has been extensively documented in many excitable tissues (for reviews, see Nicoll et al., 1990; Catterall, 1992). Although such modulations have been mostly described for potassium and calcium currents, a growing number of reports have now pointed out that voltage-gated Na^+ channels could be also subjected to modulation (for review see Caterall, 1992; Cukierman, 1996). Voltage-gated Na^+ channels are responsible for the initiation and propagation of the action potential (Hille, 1992). Modulation of their activity is therefore expected to dramatically affect neuronal excitability through a modification of the threshold for generation of action potential, a reduction of action potential duration or an alteration in the frequency at which the cell is capable of generating these action potentials. Brain Na^+ channels are phosphorylated by cyclic AMP-dependent protein kinase (PKA) and protein kinase C (PKC) in vitro and in intact neurons (Costa and Catterall, 1984; Costa et al., 1982; Rossie and Catterall, 1987; Catterall, 1992), and phosphorylation by either kinase results in channel activity inhibition (Numann et al., 1991; West et al., 1991; Gershon et al., 1992; Li et al., 1992; Smith and Goldin, 1992; Li et al. 1993; Hebert et al., 1994; Schiffmann et al., 1995; Smith and Goldin, 1997; Cantrell et al., 1997). For instance, in striatal neurons, stimulation of dopamine D_1 receptors inhibits voltage-gated Na^+ currents (Surmeier et al., 1992; Schiffmann et al., 1995) through an increase in cAMP and the stimulation of PKA, and leads to a reduction in neuronal excitability by increasing the threshold for generation of action potentials (Schiffmann et al., 1995; Zhang et al., 1998). Na^+ currents could be also regulated through additional pathways involving arachidonic acid (Fraser et al., 1993) or inhibition of protein phosphatase (Schiffmann et al., 1998). In some circumstances, activators of PKC (Godoy and Cukierman, 1994b) or activation of PKA (Li et al. 1993) may rather increase the Na^+ current amplitude.

Peptides mapping had shown that four sites located in the cytoplasmic loop between domains I and II of the α-subunit of the Na^+ channel could be phosphorylated by PKA (Murphy et al., 1993). However, Smith and Goldin (1997) have recently demonstrated for the rat brain Na^+ channel (RIIA), that the phosphorylation of one of these sites by PKA, the serine-573, is necessary and sufficient to reduce the Na^+ current amplitude. Therefore, this suggests that only two functional states of the channel could be present in the cell following activation of PKA depending on whether the specific phosphorylation site is or is not phosphorylated.

The molecular mechanism leading to the PKA-induced reduction of whole-cell Na^+ current amplitude is poorly understood. It has been repeatedly claimed that the gating dynamics of the channel was not modified in this condition (see, for instance, the recent review of Marban et al., 1998). This statement results from the observation that the phosphorylation of brain Na^+ channels reduced the whole-cell current amplitude without significantly affecting the voltage dependence of the current–voltage relationship, the voltage dependence of the steady-state activation and inactivation,

Received for publication 28 September 1998 and in final form 8 April 1999.

Address reprint requests to Pablo d'Alcantara, Faculté de Médecine, Université Libre de Bruxelles, CP601, 808 route de Lennik, 1070 Bruxelles, Belgium. Tel.: 32–2-555–6408; Fax: 32–2-555–4121; E-mail: pdalcant@ulb.ac.be.

0006-3495/99/07/204/13 $2.00

the kinetics of the time-dependent inactivation, and the kinetics of recovery from inactivation (Li et al., 1992; Schiffmann et al., 1995). This interpretation has been also reinforced by the very similar shapes of current traces corresponding to control and phosphorylated conditions. Such observations suggest that phosphorylated channels could not open upon depolarization, and thus, the effect of phosphorylation would consist of an apparent decrease of the channel population capable to open. However, the analysis of single channel data clearly indicated that phosphorylated channels may open with an unchanged conductance, but with a decreased open time fraction (Li et al., 1992), suggesting that one or several gating kinetics are affected in case of channel phosphorylation by PKA.

The gating kinetics of ion channels have been described by models that assume that channels exist in a number of discrete conformational states. Several studies have proposed models describing the gating mechanism of the Na^+ channel (Armstrong, 1981; Aldrich et al., 1983; Horn and Vandenberg, 1984; Stimers et al., 1985; Patlak, 1991; Vandenberg and Bezanilla, 1991) and containing an open state and several closed and inactivated states. The decrease in open time fraction of PKA-phosphorylated channels can be due to alteration of different kinetic rate constants, alone or in combination. However, no study has fully addressed this question so far.

The aim of the present study was therefore to identify the putative modification(s) of the gating mechanism of Na^+ channels in condition of phosphorylation by PKA, through the computer fitting of a molecular model to whole-cell Na^+ currents.

MATERIALS AND METHODS

Primary culture of striatal neurons

Three- to five-day-old Wistar pups (P3–P5) (Iffacredo, Brussels, Belgium) were aseptically decapitated and brains were placed in phosphate buffered saline containing 33 mM D-glucose. After the removal of the brains from the crania, the dorsal striata were dissected in cold phosphate buffered saline-glucose. The minced striata were pooled and gently triturated using fire-polished Pasteur pipettes. The resulting suspension was allowed to settle to remove cellular debris and the supernatant was again gently triturated. Cells were then plated on 35 mm petri dishes containing coverslips at a density ranging between 0.8 and 1 $\times$ 10^6 cells per dish. Coverslips inside petri dishes had been previously coated with 1.5 μg/mL polyornithine, rinsed with sterile water and thereafter coated with 3 μg/mL laminin. The culture medium consisted of Eagle's minimal essential medium supplemented with sodium bicarbonate (2.2 g/L), L-glutamine (0.73 g/L), glucose (3.6 g/L), penicillin (100 U/mL), streptomycin (100 μg/mL) and 10% horse serum. Two days after plating, cytosine arabinoside (2 μM) was added to the medium to prevent non-neuronal proliferation. Cultures were maintained in a humid, 5% CO_2 atmosphere at 37°C and half of the medium was changed once a week. Culture medium and sera were obtained from Gibco; all other salts and drugs were purchased from the Sigma Chemical Company (St. Louis, MO).

Whole-cell voltage-clamp recording of the sodium current

Striatal neurons 6 to 15 days in vitro were recorded using the tight-seal whole-cell mode of the patch-clamp technique (Hamill et al., 1981) with a high-gain voltage-clamp amplifier (Visual-Patch 500, Bio-logic, Claix, France). For recording, the coverslip supporting the cultured neurons was fixed on the stage of an inverted Nikon Diaphot 200 microscope (Nikon, Namur, Belgium). Patch pipettes were fabricated from borosilicate capillary tubing (1.0 mm OD borosilicate tubing, GC100F-10, Clark Electrical Instruments, Reading, UK) and pulled on a P-2000 micropipette puller (Sutter Instrument Co., Novato, CA). They presented resistances of 2.5–8 MΩ when filled with the patch pipette solution (see below). Junction potential between the electrode solution and the bath was adjusted to zero, and membrane potential values were not corrected with respect to this liquid junction potential. Series resistances and cell capacitances were compensated using the procedure described in the Visual Patch 500 manual.

Membrane currents were filtered using an inbuilt five-pole Bessel low-pass filter at 5 kHz of the Visual Patch 500, and each current trace was an average of two consecutive records elicited at 0.7 Hz.

Patch-clamp experiments were conducted at room temperature (21–24°C). To isolate the sodium current, the extracellular recording solution contained 50 mM NaCl, 100 mM tetraethylammonium chloride, 1 mM $MgCl_2$, 1 mM CaCl2, 1 mM $CoCl_2$, 5 mM $CsCl_2$, 10 mM D-glucose, and 10 mM HEPES adjusted to pH 7.3 and 295–330 mOsmol/L. The pipette solution contained 65 mM di(Tris)phosphate, 40 mM Tris-base, 5 mM CsCl, 11 mM EGTA, 1 mm $CaCl_2$, 1 mM $MgCl_2$, 0.4 mM Na_3GTP, 4 mM Na_2ATP, 0.2 mM cAMP, 20 mM phosphocreatine, 50 U/mL creatine phosphokinase, 0.1 mM leupeptin, 10 mM D-glucose, and 10 mM HEPES adjusted to pH 7.3 and 260–275 mOsmol/L. To reach the gigaseal cell-attached configuration, the tip of the pipette was back-filled with the intracellular solution without creatine phosphokinase, leupeptin, phosphocreatine in all experiments.

Depending on experimental protocols, the basic solutions were modified by addition of compounds and drugs. Forskolin and 1,9-dideoxyforskolin (RBI, Natick, MA) dissolved in ethanol at 10 mM were added to the bath solution to give the adequate final concentration (50 μM). Bath solutions were exchanged using the Watson Marlow 205U pump (Watson Marlow, Leuven, Belgium).

Previous published data demonstrating the effects on Na^+ current of PKA and phosphorylated DARPP-32, an inhibitor of protein phosphatase 1, as well as its inactive form, non-phosphorylated DARPP-32 (Schiffmann et al., 1995; Schiffmann et al., 1998) were also analyzed as described below.

Data analysis

Na^+ current traces experimentally obtained (as shown, for instance, in Fig. 1 *A*) were analyzed by curve fitting (nonlinear regression based on Marquardt–Levenberg algorithm) using a model describing the gating mechanism of the Na+ channel, as follows. The model, defined by kinetic transitions between different channel states (closed, open, or inactivated), was mathematically described by a system of first order differential equations

$$\frac{dX_i}{dt} = \sum_{i \neq j}^{n} k_{ji} X_j - \sum_{i \neq j}^{n} k_{ij} X_i, \quad (1)$$

where X_i was the fraction of channel population in state i, and k_{ij} was the first order kinetic constant characterizing the conversion of state i to state j. These differential equations were numerically integrated by using Runge–Kutta algorithm. Thus, this procedure gave the time course of the fraction of channel population in the open state, i.e., the open probability $P_o(t)$. To fit the model to the experimental data, the measured Na^+ current (I) had to be numerically transformed in open probability, using the theoretical relationship

$$I(t) = iNP_o(t), \quad (2)$$

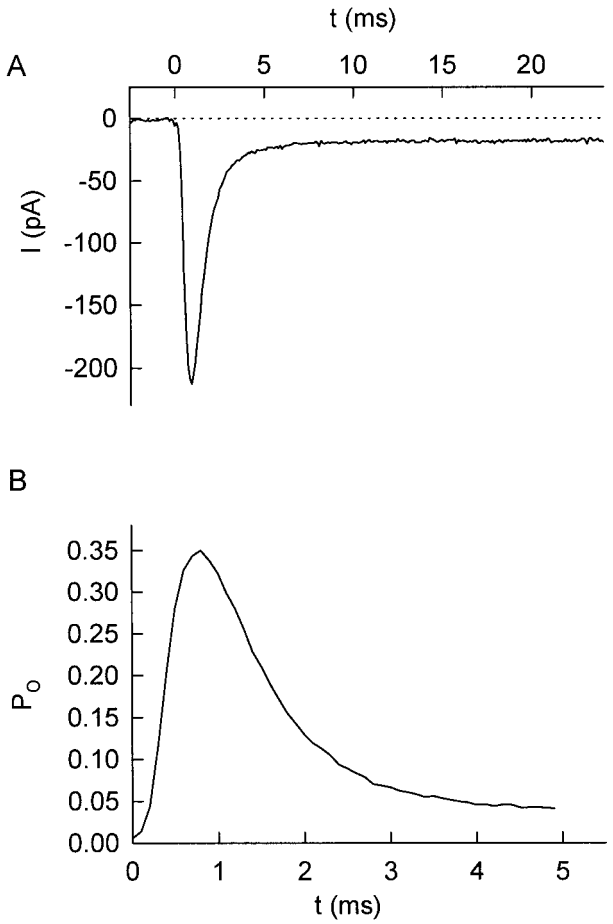

FIGURE 1 The Na^+ current of striatal neurons in primary culture. (*A*) In voltage-clamp and in conditions allowing the isolation of Na^+ currents, depolarizing voltage step from a holding potential of −80 mV to a potential of 0 mV, evoked an inward current. (*B*) Open probability of the Na^+ channel, corresponding to the normalized Na^+ current for which the open probability peak is fixed at 0.35 (the scaling factor *S*, as defined in Eq. 4, is equal to −608 pA).

where *N* and *i* referred to the total number of channels and to the current of a single open channel, respectively. Practically, the value of the scaling factor *iN* could not be determined, because *N* was unknown in our experiments. To circumvent this problem, we have referred to studies showing the voltage and time dependencies of the open probability (Patlak, 1991), and assumed that, at a chosen membrane potential, the maximal open probability with respect to time ($P_{o,max}$) corresponded to the peak amplitude of Na^+ current (I_{max}). Thus, the normalization

$$P_o(t) = I(t)/S \tag{3}$$

with

$$S = I_{max}/P_{o,max} \tag{4}$$

was applied. For instance, the curve $I(t)$ (Fig. 1 *A*) which was obtained using a depolarization step from −90 mV to 0 mV, was transformed in the curve $P_o(t)$ (Fig. 1 *B*) using a $P_{o,max}$ of 0.35 (Patlak, 1991). The kinetic parameters k_{ij} of the model were estimated by an iterative procedure searching for the set of parameter values generating the minimal deviation (least square fitting) between the experimental curve $P_o(t)$ and the theoretical curve given by numerical integration of the differential equations.

Statistical analysis

To compare the parameter estimates corresponding to the curves obtained in control and phosphorylation conditions, we used a two-tailed paired *t*-test and considered the difference significant if $p < 0.05$.

RESULTS

Gating mechanism modeling

Several studies have proposed models describing the gating mechanism of the Na^+ channel (Armstrong, 1981; Aldrich et al., 1983; Horn and Vandenberg, 1984; Stimers et al., 1985; Patlak, 1991; Vandenberg and Bezanilla, 1991). Generally, these models contained several closed and inactivated states. Preliminary simulations indicated that our experimental data required the presence of at least three closed states, one open state, and two inactivated states. In fact, models with one or two closed states were not able to accommodate quantitatively the delayed activation of the channel causing the apparent lag in the current onset subsequent to depolarization; likewise, one inactivated state was not sufficient to account for the apparent existence of two kinetic components in the relaxation of Na^+ current during the depolarization. This description was in general accordance with several proposed models based on the existence of three closed states (Vandenberg and Bezanilla, 1991) and two inactivated states (Patlak, 1991; Sarkar et al., 1995). Furthermore, it has been repeatedly suggested that the inactivation of a channel was not necessarily preceded by its opening (Bean, 1981; Horn et al., 1981; Vandenberg and Horn, 1984; Goldman 1995). The minimal model compatible with our data and in good agreement with the literature could be qualitatively described by

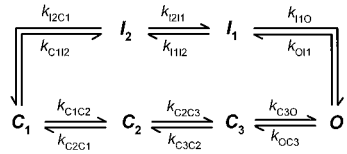

Model 1

Definition of an operational model

Preliminary analyses of the proposed minimal scheme revealed acute over-parametrization of this model, in the sense that several parameters were highly correlated when the fitting procedure was applied to the experimental data. A dependence was clearly observed among the different kinetic parameters of the activation pathway, and between the parameters of the two inactivation pathways. Therefore, to eliminate these parameter dependencies, we have simplified the model in several respects by introducing some constraints, as follows.

Simplification of the activation pathway

Many studies dealing with single channel experiments concluded that there existed a sequence of transitions between

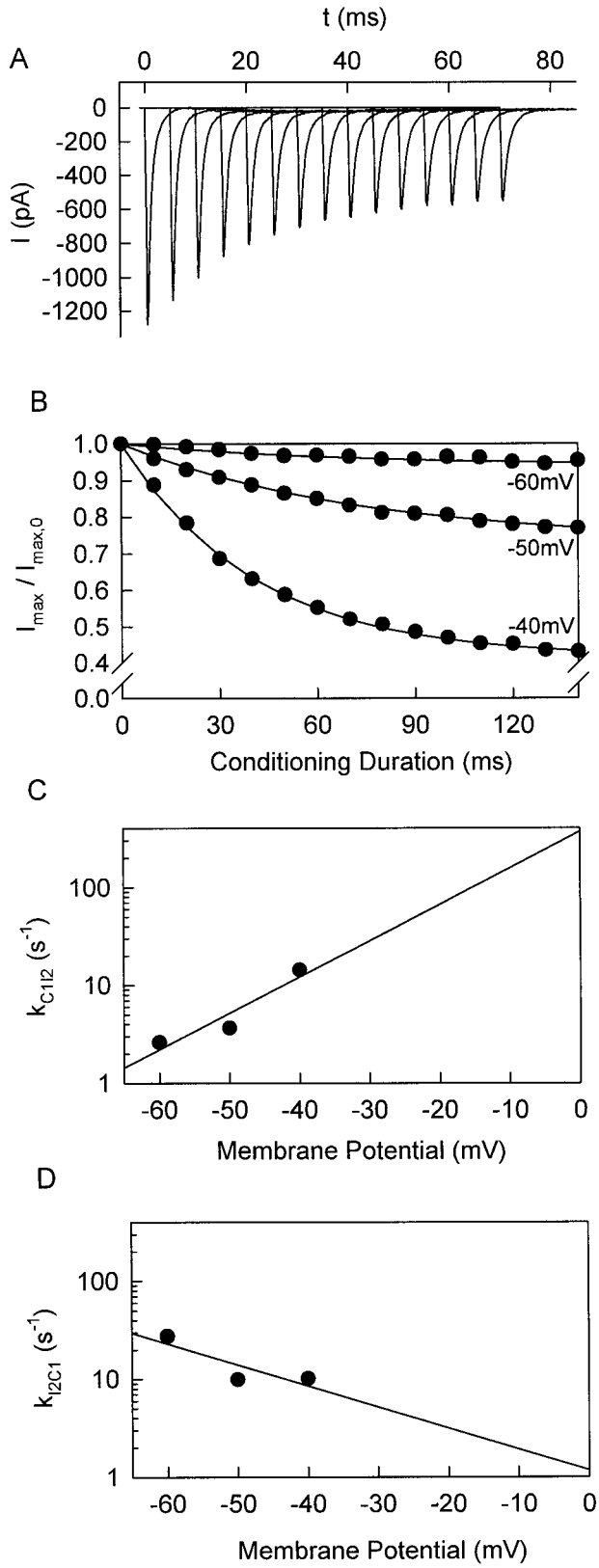

FIGURE 2 Characterization of the inactivation from closed states. (*A*) The experimental conditions were: holding potential = −90 mV; conditioning potential = −40 mV; test pulse potential = 0 mV. The different traces of Na^+ current begin at the initiation of the conditioning pulse (t = 0), and correspond to increasing durations of the conditioning pulse. (*B*) Inactivation from closed states for three different conditioning potentials. (●) normalized peak of the average current during the test pulse; the lines represent the fitting of Eq. 5 to the points. (*C*, *D*) (●) Estimates of the kinetic parameters k_{C1I2} and k_{I2C1} for the three different potentials. The lines represent the fitting of Eq. 6 to the points.

closed states before channel opening. This sequence would reflect the process of effective charge transfer (Lauger et al., 1980; Hirschberg et al., 1995; Sigworth, 1995; Sigg and Bezanilla, 1997). As proposed in other theoretical studies (Vandenberg and Bezanilla, 1991), the kinetic constants of several transitions among some of the different closed states might be equalized. Such a hypothesis did not mean that these constants were actually equal, but merely reflected the fact that the experimental data were not informative enough for individually estimating these constants, and thus, we simplified the activation pathway by equating all the kinetic constants of the transitions leading to the open state ($k_{C1C2} = k_{C2C3} = k_{C3O}$), and by neglecting the reverse transitions between closed states ($k_{C2C1} = k_{C3C2} = 0$).

Characterization of the transition between closed and inactivated states

It was impossible to estimate, from a single experimental trace, the kinetic parameters of both inactivation pathways, because of their mutual dependence. Therefore, we tried to characterize independently the kinetics of inactivation from closed states by using the experimental protocol proposed by Aldrich and Stevens (1983) and, more recently, used by Goldman (1995). It consisted of a sequence of two successive potential pulses: the first pulse (conditioning pulse) was done at variable durations and at low potential (ranging from −60 mV to −40 mV), in such a manner that inactivation might develop from the closed state without any channel opening; the second pulse (test pulse), which immediately followed the conditioning pulse, produced a current trace with a peak amplitude proportional to the number of channels that were not inactivated by the conditioning pulse, thus, still in the closed state. The quantitative analysis of the relationship between the peak amplitude and the duration of the conditioning pulse allowed the characterization of the kinetic of transition between closed and inactivated states. The result obtained with a holding potential of −90 mV, a conditioning potential of −40 mV and a test potential of 0 mV is shown in Fig. 2 *A*: the different traces of Na^+ current begin at the initiation of the conditioning pulse (t = 0), and correspond to increasing durations of the conditioning pulse. For each duration, the peak amplitude produced by the test pulse was divided by the peak amplitude obtained in the absence of conditioning pulse (peak of the first trace). This ratio was plotted as a function of the conditioning duration, and for the three conditioning potentials used (Fig. 2 *B*). It appeared that the closed state inactivation followed monoexponential kinetics, as observed by

Goldman (1995). The simplest way to account for the observed kinetics was to consider that, assuming that the whole channel population was in the state C_1 at the holding potential of −90 mV, the conditioning pulse only induced a reversible transition between C_1 and the inactivated state I_2. The kinetic equation governing such a mechanism was

$$C_1(t) = \frac{k_{I2C1}}{(k_{C1I2} + k_{I2C1})} + \frac{k_{C1I2}}{(k_{C1I2} + k_{I2C1})} \cdot \exp[-(k_{C1I2} + k_{I2C1}) \cdot t]. \quad (5)$$

The least square fitting of this equation to the three curves led to estimates of the two parameters k_{C1I2} and k_{I2C1} in the three conditions. These estimates were plotted against the conditional potential to calculate, by extrapolation, the parameter values at higher potentials (Fig. 2 *C* and *D*). This extrapolation was done according to Stevens' (1978) method, which assumed an exponential relationship between a kinetic parameter k and the membrane potential V

$$k(V) = A \cdot \exp(qFV/RT), \quad (6)$$

where q is the effective valence of the transition rate, F is the Faraday constant, R is the gas constant, and T is the absolute temperature. Fitting this exponential equation to a set of kinetic parameter estimates led to the determination of A and qF/RT. The exponential equation was then used to calculate the extrapolated values of k_{C1I2} and k_{I2C1} at the potential applied in the standard experiments, which ranged from −20 mV to 0 mV. It must be stressed that, for these potentials, the k_{C1I2} estimate was much higher than the k_{I2C1} estimate, and thus, the transition from C_1 to I_2 might be considered, in these conditions, as an irreversible process.

This first part of the work allowed the definition of the operational model,

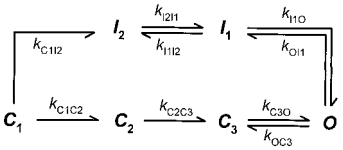

Model 2

which was used for the fitting of the $P_o(t)$ curve obtained from the time course of the current $I(t)$ by using Eq. 3. For instance, an experimental trace was analyzed on the basis of this operational model. The six unknown independent parameters were estimated by the described fitting procedure, $k_{C3O}(= k_{C1C2} = k_{C2C3}) = 8070\ s^{-1}$, $k_{OC3} = 0.027\ s^{-1}$, $k_{OI1} = 4411\ s^{-1}$, $k_{I1O} = 816\ s^{-1}$, $k_{I1I2} = 819\ s^{-1}$, and $k_{I2I1} = 44\ s^{-1}$. The corresponding fitted curve is shown in Fig. 3.

The same strategy had to be applied to current curves obtained in different conditions to explain the effect of channel phosphorylation on the gating mechanism.

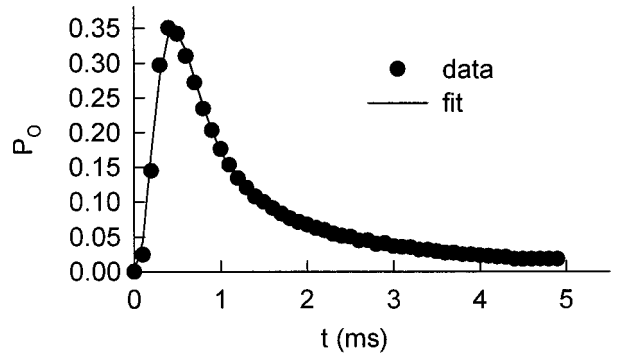

FIGURE 3 Fitting of Model 2 to the experimental data (scaling factor $S = -3814$ pA). Data record for a test pulses to 0 mV from a holding potential = −90 mV. The parameter estimates are $k_{C1C2} = k_{C2C3} = k_{C3O} = 8070\ s^{-1}$, $k_{OC3} = 0.027\ s^{-1}$, $k_{OI1} = 4411\ s^{-1}$, $k_{I1O} = 816\ s^{-1}$ $k_{I1I2} = 819\ s^{-1}$, and $k_{I2I1} = 44\ s^{-1}$.

Effect of forskolin-induced channel phosphorylation

In agreement with previous results describing the partial inhibitory effect of PKA on Na^+ channel activity (Gershon et al., 1992; Li et al., 1992; Smith and Goldin, 1992; Li et al. 1993; Hebert et al., 1994; Schiffmann et al., 1995; Smith and Goldin, 1997, Cantrell et al., 1997), the addition of forskolin (50 μM) in the bath depressed by 18% (mean of 10 independent observations) the peak amplitude of Na^+ current evoked by a −90 mV to 0 mV step depolarization (see representative curves in Figs. 4 *A* and 6 *A*). This effect was reversed upon wash-out and was statistically significant ($p < 0.05$) as compared to that of the inactive analog 1,9-dideoxy-forskolin ($n = 5$), which did not affect the Na^+ current amplitude (Fig. 4 *B*).

The putative effect of forskolin on steady-state inactivation and activation curves was investigated. The activation curve was constructed from the current-voltage curves obtained by applying 15 ms depolarizing pulses from a holding potential of −90 mV by 10 mV steps. The activation curve was obtained using the equation

$$G = I_{max}/(V - E_{rev}), \quad (7)$$

where E_{rev} is the extrapolated reversal potential from the current–voltage curve, and G is the macroscopic conductance. The calculated conductances were normalized, plotted as a function of the test potential (Fig. 4 *C*) and the curves were fitted by the Boltzmann equation,

$$G/G_{max} = 1/\{1 + \exp[(V_h - V)/k]\}, \quad (8)$$

where V is the test potential, V_h is the voltage at half maximal activation, and k is the slope factor. The application of forskolin did not significantly modify the voltage-dependent activation parameters (Fig. 4 *D*).

The voltage-dependent steady-state inactivation was analyzed using a two-pulse protocol. The potential was held during 30 ms, successively from −120 to +20 mV before application of a constant test pulse to 0 mV. The steady-

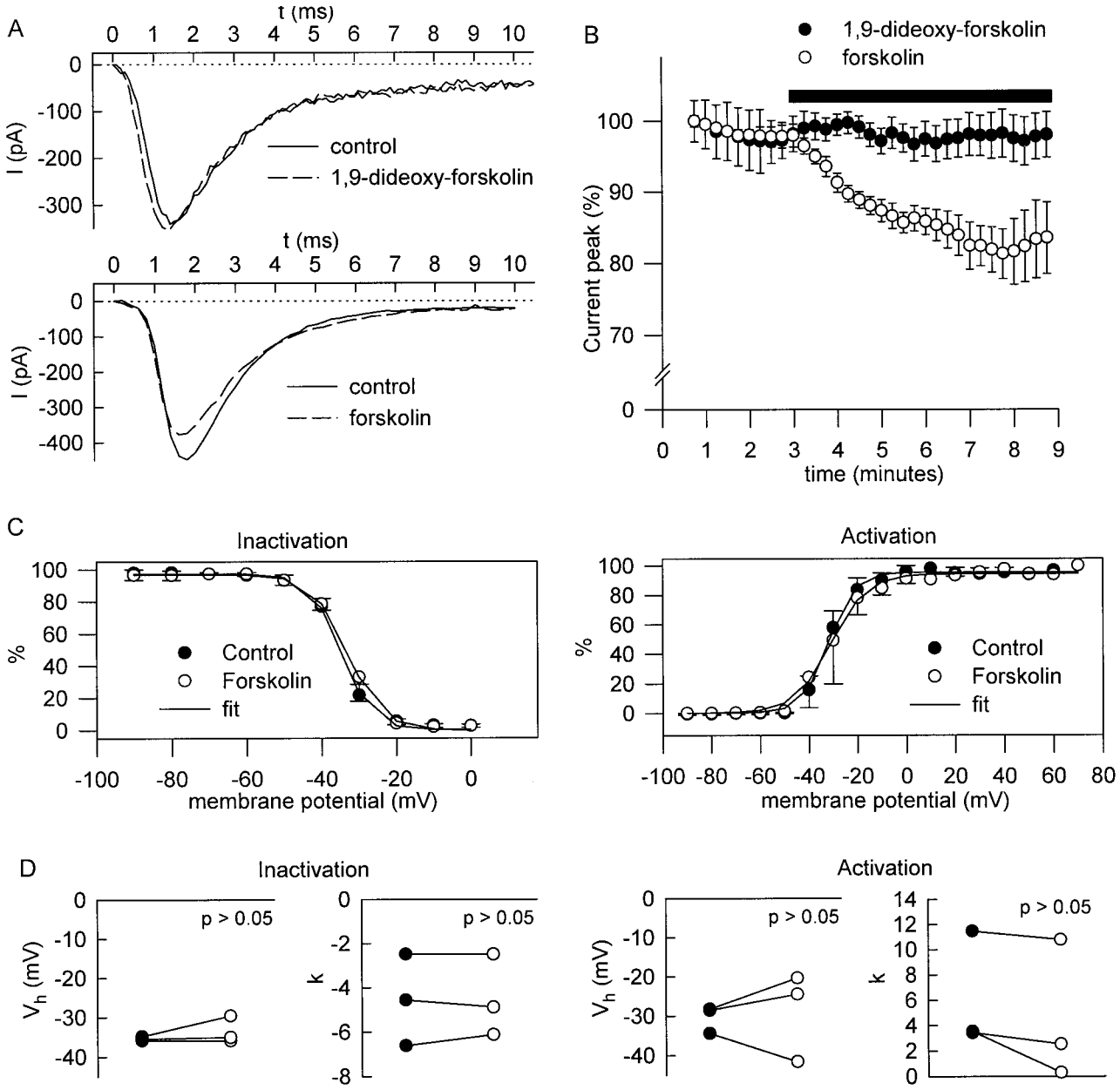

FIGURE 4 Effect of forskolin and 1,9-dideoxy-forskolin on voltage-gated sodium current, and effect of forskolin on steady-state inactivation and activation curves. (*A*) Typical experimental traces obtained either in the presence of forskolin or in the presence of the inactive analogue 1,9-dideoxy-forskolin. Holding potential = −90 mV; test pulse potential = 0 mV. (*B*) Normalized peak Na^+ (mean ± SE, n = 3 to 5) during a 6-min application of 1,9-dideoxy-forskolin and forskolin (*solid bar*). (*C*) Activation and steady-state inactivation curves (fitted by Boltzmann equation (Eqs. 8 and 9)) were obtained before (●) and after (○) application of forskolin (n = 3). (*D*) Scatter plots of V_h (potential at mid-point) and k (slope factor) values for individual neurons show that forskolin did not significantly modify ($p > 0.05$) either the steady-state inactivation [V_h (control) = −35.3 ± 0.3 mV; V_h (forskolin) = −33.5 ± 2.0 mV; k(control) = −4.6 ± 1.2; k(forskolin) = −4.5 ± 1.1) or activation (V_h (control) = −30.4 ± 2.0 mV; V_h (forskolin) = −28.8 ± 6.5 mV; k (control) = 6.2 ± 2.7; k (forskolin) = 4.6 ± 3.2].

state inactivation curve was determined by normalizing the peak amplitude of the sodium current during the test pulse as a function of the conditioning potential (Fig. 4 *C*). These curves were fitted by the Boltzmann equation,

$$G/G_{max} = 1/\{1 + \exp[(V_h - V)/k]\}, \quad (9)$$

where V is the conditioning potential, V_h is the voltage at half maximal inactivation, and k is the slope factor. The application of forskolin did not significantly modify the steady-state inactivation parameters (Fig. 4 *D*).

If channel phosphorylation exerted its effect through modulation of one or several transition kinetic parameters, the statistical comparison of the parameter estimates resulting from the fitting of the curves obtained with control and forskolin treated cells should be able to identify the state transition that was sensitive to phosphorylation. Before try-

ing to fit the operational model to these curves, it was necessary to analyze the possible effect of phosphorylation on the inactivation of the closed channel.

Forskolin effect on the inactivation of the closed channel

The experimental protocol leading to the estimate of k_{C1I2} and k_{I2C1} was applied as described in Fig. 2, both in the control condition and after completion of forskolin-induced phosphorylation. Figure 5 *A* shows a representative result obtained with a conditioning potential of −50 mV. In this case, forskolin seemed to have little effect, if any, on the inactivation of the closed channel. In fact, no significant difference (paired *t*-test, $n = 5$) was observed between the parameter estimates obtained in the absence and in the presence of forskolin (Fig. 5, *B* and *C*).

Characterization of forskolin effect on the gating mechanism

Because the k_{C1I2} parameter was insensitive to forskolin-induced phosphorylation of the Na^+ channel, the same parameter value was considered for fitting the model to control and forskolin curves, and was estimated according to the extrapolation method described in Fig. 2 *C*. Figure 6 *B* shows the fitting of the two curves obtained in one representative experiment out of nine. The forskolin-induced modification of the parameter values (Fig. 6 *C*) was analyzed by paired *t*-test, which indicated that only the parameter k_{OI1} was significantly increased ($p = 0.0016$). Fitting of current traces obtained at the beginning and the end of the recording (2–3 min and 8–10 min after reaching the whole-cell recording configuration, respectively) of 1,9-dideoxy-forskolin-treated neurons and neurons bathed in a standard saline solution showed no significant change in the parameter estimates in these conditions (data not shown).

On the basis of this analysis, we conclude that the partial inhibition of the channel activity due to PKA-induced phosphorylation should result from an accelerated inactivation from the open state.

Analysis of the effect of channel phosphorylation directly induced by PKA

To confirm the results obtained with forskolin-induced phosphorylation, previously recorded current traces (Schiffmann et al., 1995), for which the phosphorylation was induced by the PKA catalytic subunit diffusing from the patch-pipette, were revisited. It must be noted that, for these experimental results, we were not able to estimate the individual k_{C1I2} parameters, because the required protocol (Aldrich and Stevens, 1983; Goldman, 1995) was not applied at the time the traces were recorded; therefore, we extrapolated a k_{C1I2} value at the correct test potential from the averaged k_{C1I2} estimates found with the forskolin-treated cells. Figure 7 shows the results obtained from −80 mV to −20 mV depolarization experiments. The analysis of a total of six

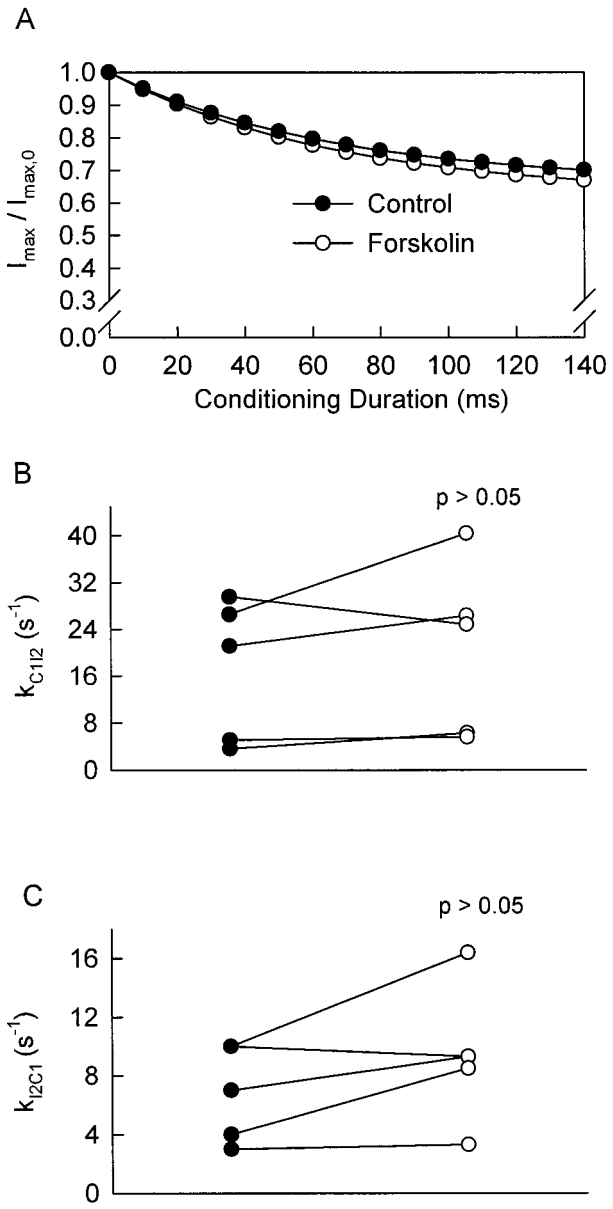

FIGURE 5 Effect of phosphorylation on the inactivation from closed states. The experimental protocol is the same as in Fig. 2. (*A*) Holding potential = −90 mV; conditioning potential = −50 mV; test pulse potential = 0 mV. The peak of the average current during the test pulse is shown as a function of conditioning duration. Closed and open circles refer to control and forskolin treated cells, respectively. (*B*, *C*) Scatter plots of paired k_{C1I2} and k_{I2C1} values for individual neurons. Paired *t*-test indicates no significant difference between the two situations.

records confirmed that only the k_{OI1} parameter was significantly increased ($p = 0.017$).

Analysis of the effect of the phosphatase inhibitor phospho-DARPP-32

The endogenous inhibitor of protein phosphatase 1, phosphorylated DARPP-32, has been demonstrated to reduce the Na^+ current peak amplitude when loaded in neurons by

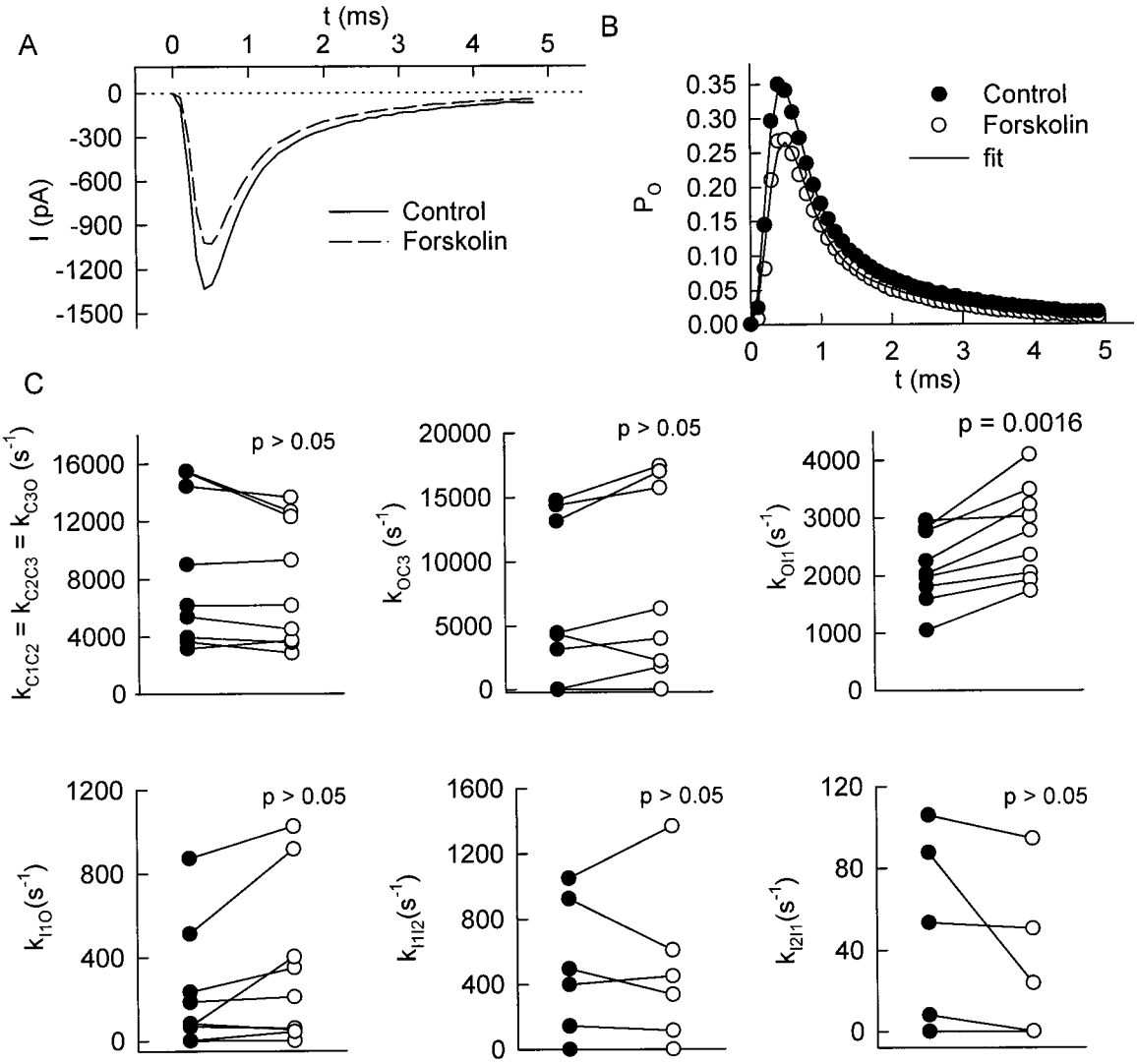

FIGURE 6 Analysis of experimental traces (out of nine) obtained in the absence (●) or in the presence (○) of forskolin. (*A*) Typical experimental traces showing forskolin-induced current reduction. Holding potential = −90 mV; test pulse potential = 0 mV. (*B*) Open probability time course was calculated using a scaling factor $S = -3814$ pA. (*C*) Effect of forskolin-induced phosphorylation on the kinetic parameters. Scatter plots of k_{C1C2}, k_{C2C3}, k_{C3O}, k_{OC3}, k_{OI1}, k_{I1O}, k_{I1I2}, and k_{I2I1} values for nine individual neurons. Only k_{OI1} exhibits a significant increase due to the forskolin treatment.

diffusion from the patch pipette (Schiffmann et al., 1998). It has been proposed that this effect was mediated by an increase of the phosphorylation level of the Na^+ channel. If this phosphorylation partially or totally involved the basal activity of PKA, one can expect that the addition of phospho-DARPP-32 might have an effect on the gating mechanism similar to the one obtained with the catalytic unit of the kinase A, i.e., an increase of k_{OI1}. To test this prediction, previously obtained current traces (Schiffmann et al., 1998) were analyzed (Fig. 8). It appeared that only the k_{OI1} parameter was significantly changed in the presence of phospho-DARPP-32 ($n = 3, p = 0.019$), suggesting that in basal condition and in the case of phosphatase inhibition, PKA was the major active kinase. However, this effect was apparently less pronounced than when PKA was added, possibly because either phospho-DARPP-32 would lead to a lower phosphorylation level than added PKA, or other kinase(s) would also take a minor but significant part in the phosphorylation process. Fitting of current traces obtained at the beginning and the end of the recording (2–3 min and 8–10 min after reaching the whole-cell recording configuration, respectively) of nonphospho-DARPP-32-loaded neurons showed no significant change in the parameter estimates (data not shown).

DISCUSSION

The inhibitory effect of PKA-induced phosphorylation of the Na^+ channel has been widely documented (Gershon et al., 1992; Li et al., 1992; Smith and Goldin, 1992; Li et al. 1993; Hebert et al., 1994; Schiffmann et al., 1995; Smith and Goldin, 1997, Cantrell et al., 1997). Several potential sites of phosphorylation have been identified (Murphy et al.,

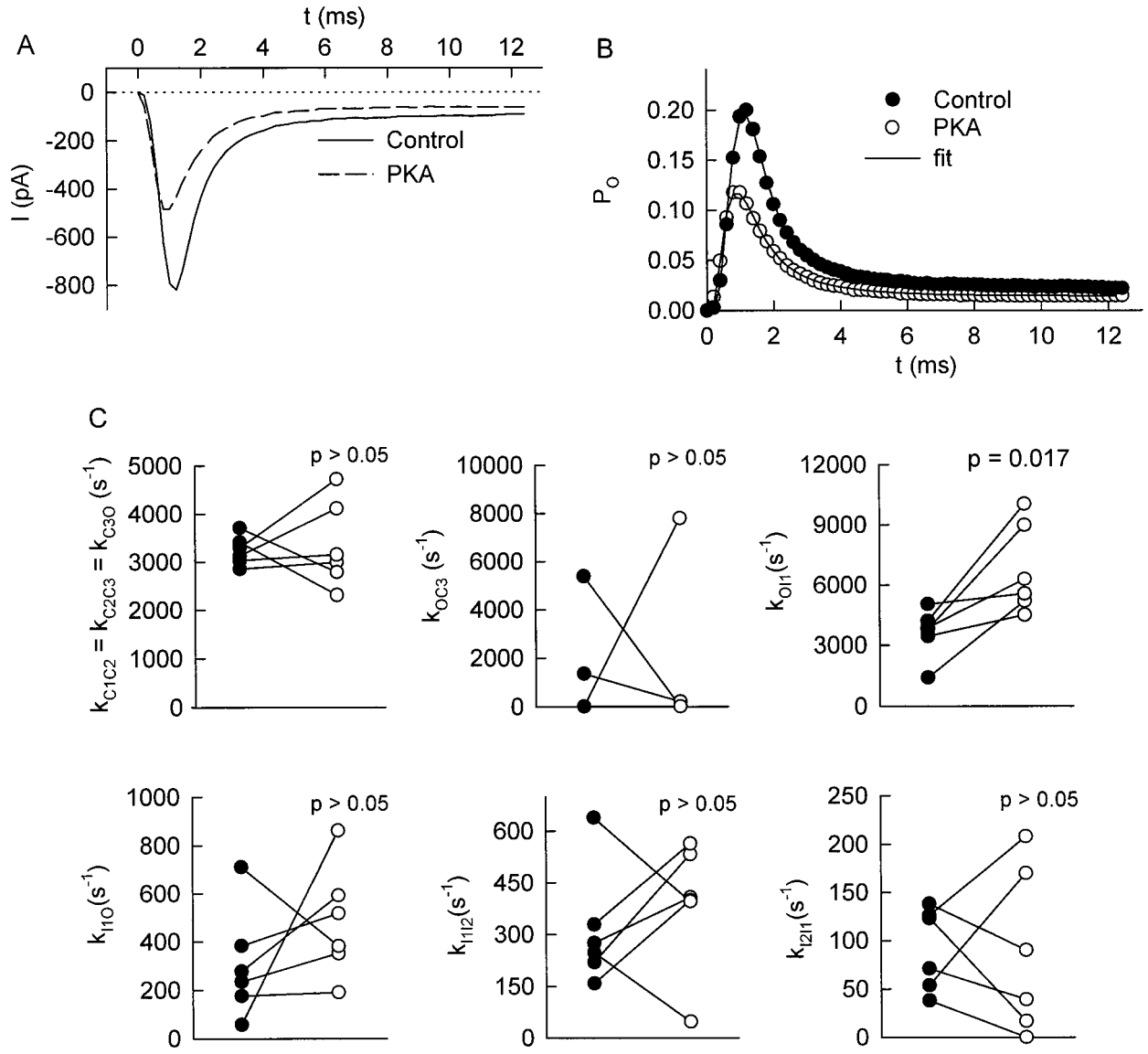

FIGURE 7 Analysis of experimental traces obtained with (○) or without (●) the addition of the PKA catalytic unit. (*A*) Typical experimental traces (out of six) showing PKA-induced current reduction. Holding potential = −80 mV; test pulse potential = −20 mV. (*B*) Open probability time course was calculated using a scaling factor $S = -4102$ pA. (*C*) Effect of PKA-induced phosphorylation on the kinetic parameters. Scatter plots of k_{C1C2}, k_{C2C3}, k_{C3O}, k_{OC3}, k_{OI1}, k_{I1O}, k_{I1I2}, and k_{I2I1} values for six individual neurons. Only k_{OI1} exhibits a significant increase due to the addition of PKA catalytic unit.

1993). It now appears that the phosphorylation of only one of them is sufficient to induce channel inhibition (Smith and Goldin, 1997). The study of the inhibitory effect of PKA-induced phosphorylation of Na^+ channels in excised membrane patches (Li et al., 1992) suggests that the reduction in Na^+ current must be attributed primarily to reduction of the open probability. On one hand, null sweeps represent about 20% and 50% of the records before and after phosphorylation, respectively. On the other hand, the total channel open time during the stimulating pulse in responding sweeps significantly decreases by a factor of about 2.6 after phosphorylation (maximum likelihood fitting of the data taken from Fig. 2 *C* in Li et al., 1992). Thus, when the phosphorylated channel opening can be detected and measured, it is characterized by a lower half life as compared to the one observed in the control situation.

The results presented in our study, which assumes that the phosphorylated channel exhibits modified gating kinetics, indicate that the phosphorylation-induced decrease in whole-cell Na^+ current is explained by a faster channel inactivation, leading thus to a lower mean open time as observed in single channel experiments. The minimal operational model used to demonstrate this point is compatible with the current knowledge on the gating mechanism of the Na^+ channel. It considers two inactivating pathways: an inactivated state is formed either from a closed state, or from an open state. Direct observation presented in this work shows that channel phosphorylation would not modify

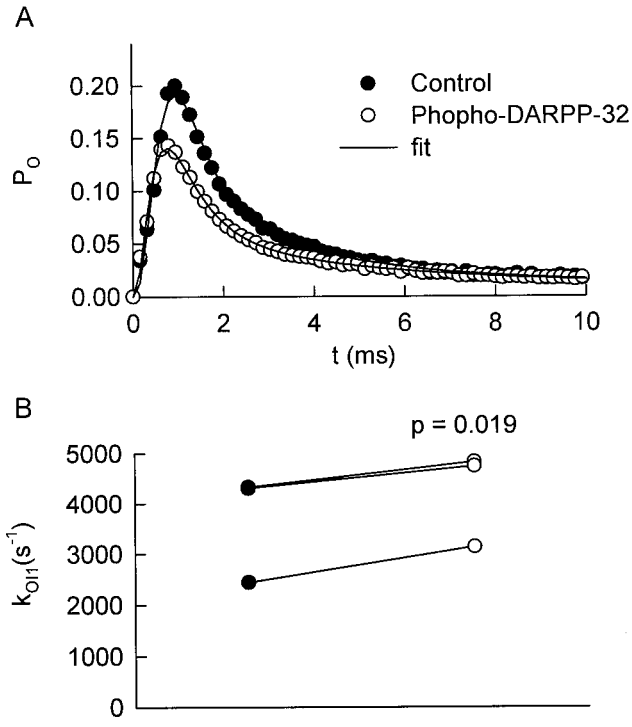

FIGURE 8 Analysis of experimental traces obtained at the beginning (●) or the end (○) of recordings of phospho-DARPP-32 loaded neurons. (*A*) Open probability time course was calculated using a scaling factor $S = -2661$ pA. Holding potential = −80 mV; test pulse potential = −20 mV. (*B*) Effect of the addition of phospho-DARPP32 on the kinetic parameters. Scatter plots of k_{C1C2}, k_{C2C3}, k_{C3O}, k_{OC3}, k_{OI1}, k_{I1O}, k_{I1I2}, and k_{I2I1} values for three individual neurons. Only k_{OI1} exhibits a significant increase due to the addition of phospho-DARPP-32.

the kinetics of inactivation from the closed state. On the contrary, the statistical analysis of the quantitative characterization by curve fitting suggests that, within the framework of this model, the O to I_1 transition is significantly faster when the channel is phosphorylated. No significant difference was detected with the other kinetic parameters. A typical figure of the factor by which k_{OI1} is multiplied due to channel phosphorylation is 2. However, it has been proposed that, under control conditions, the Na^+ channel population would not be completely unphosphorylated, because more channel activity was elicited when the phosphorylation level was decreased (Gershon et al., 1992; Li et al., 1992). Therefore, the given k_{OI1} estimates would rather characterize average situations corresponding to different levels of phosphorylation.

It must be stressed that the increased number of null sweeps obtained with excised membrane patches after phosphorylation (Li et al., 1992) can be entirely accounted for by a decreased mean open time of the channel, without any change in the number of openable channels. Assuming a mean open time of 0.23 ms in the control condition and an effective minimal duration of detectable openings of 0.15 ms (see the characterization of the wild type channel in McPhee et al., 1995; Horn and Vandenberg, 1984), a simple calculation based on the exponential distribution of the open times indicates that 48% of the openings are not detectable, leading to 23% of null sweeps if there are two channels in the patch (as suggested in Fig. 1 in Li et al., 1992). A similar calculation shows that, if channel phosphorylation decreases the mean open time by a factor of two, 53% of null sweeps are generated with a 2-channel patch: these figures for the expected number of null sweeps satisfactorily account for the values reported by Li and co-workers (1992). These simple calculations based on realistic experimental characteristics demonstrate that it is not necessary to invoke a phosphorylation-induced decrease of the number of openable channels for explaining the increased number of null sweeps.

The operational model was simulated by using typical parameter values obtained in this work. The two curves corresponding to control and phosphorylation conditions, respectively, were generated with the same parameter values except k_{OI1}, which was multiplied by a factor of 2 (Fig. 9 *A*). The two curves exhibit very similar shapes, as if they only differ in first approximation by a simple scaling factor. A possible intuitive interpretation, as previously proposed in the literature, is that channel phosphorylation would deplete the population of channels capable to open upon depolarization through an inactivation from the closed state. Interestingly, this interpretation can be supported by the analysis of experimental curves on the basis of a minimal model of Hodgkin–Huxley (1952) type compatible with our data. Indeed, when the six pairs of curves obtained in the experiments using PKA were fitted by the HH model (referring to a third-order activation process and a biexponential inactivation process),

$$I_{Na+}(t) = I_{ss} \cdot (1 - e^{t/t_m})^3 \cdot (1 + h_1 \cdot e^{t/t_1} + h_2 \cdot e^{t/t_2}), \qquad (10)$$

no systematic and significant modification was observed in parameters characterizing both activation and inactivation kinetics (Fig. 10). It would have been concluded, on the basis of such an analysis, that phosphorylation of the channel would not alter the gating mechanism of the channel. Thus, it appears now that such an empirical model is unable to detect that the inactivation of the open state is actually accelerated by the phosphorylating treatment.

Although our study suggests that the phosphorylation of the channel would induce a significant acceleration of the inactivation from the open state, it is not able to demonstrate that the other transitions actually are unaffected. However, it is interesting to see how P_o, and thus, the current trace, would transform if the Na^+ current attenuation induced by phosphorylation is due to a decrease of the activation rate. For that purpose, we simulated the model as in Fig. 9 *A*, except that the phosphorylation conditions were defined by a k_{CO} ($= k_{C1C2} = k_{C2C3} = k_{C3O}$) value divided by 1.5, leading to the same current value at the peak of the inhibited trace (Fig. 9 *B*). In agreement with other simulations (Godoy and Cukierman, 1994a), the decrease of k_{CO} has an obvious effect on the shape of the inhibited curve, which now intersects the control curve. This phenomenon results

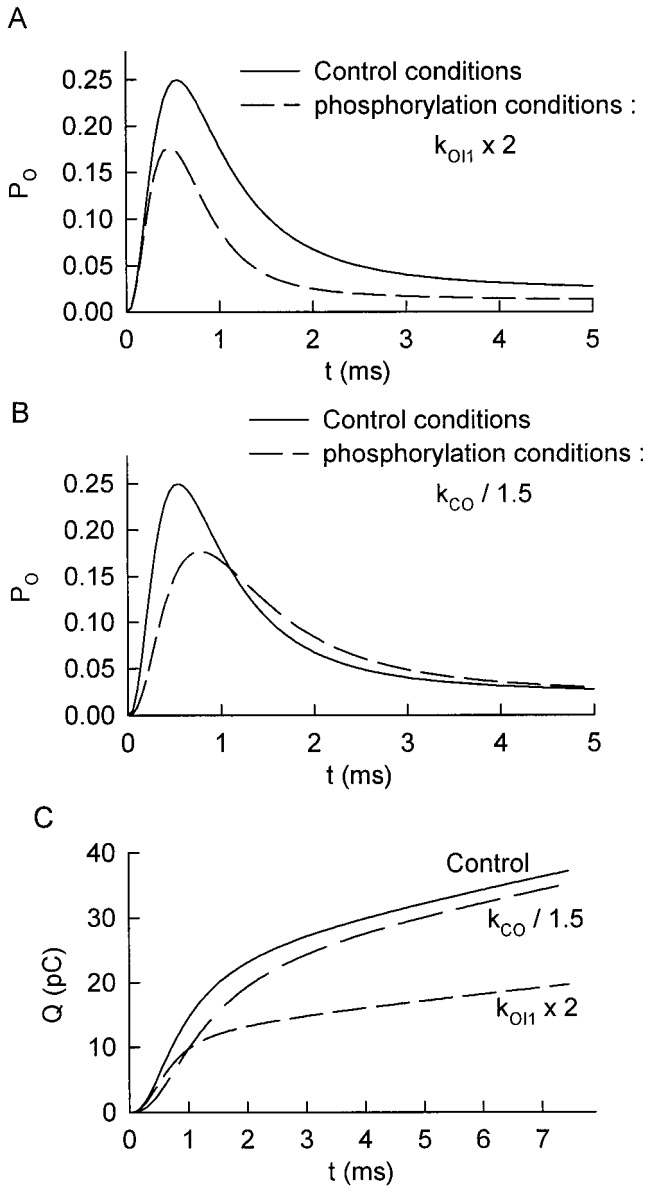

FIGURE 9 Simulation of Model 2 using typical parameter values. (*A*) The control curve was obtained using the following parameter values: $k_{C1C2} = k_{C2C3} = k_{C3O} = 6977\ s^{-1}$, $k_{OC3} = 6664\ s^{-1}$, $k_{OI1} = 3349\ s^{-1}$, $k_{I1O} = 203\ s^{-1}$, $k_{I1I2} = 389\ s^{-1}$, $k_{I2I1} = 262\ s^{-1}$, and $k_{C1I2} = 411\ s^{-1}$. The curve corresponding to the phosphorylation conditions was obtained with the same parameter values, except k_{OI1}, which was multiplied by a factor of 2, leading to a 29% reduction in the peak amplitude. (*B*) Control curve as in *A*; the curve corresponding to the phosphorylation conditions was obtained with the same parameter values, except k_{CO} ($= k_{C1C2} = k_{C2C3} = k_{C3O}$) which was divided by 1.5 to produce the same 29% reduction in the peak amplitude. (*C*) Time course of net charge accumulation in the three conditions. The net charge Q was calculated by integrating the current $I(t)$ with respect to time, after conversion of $P_O(t)$ into $I(t)$ by using a scaling factor $S = 4000$ pA.

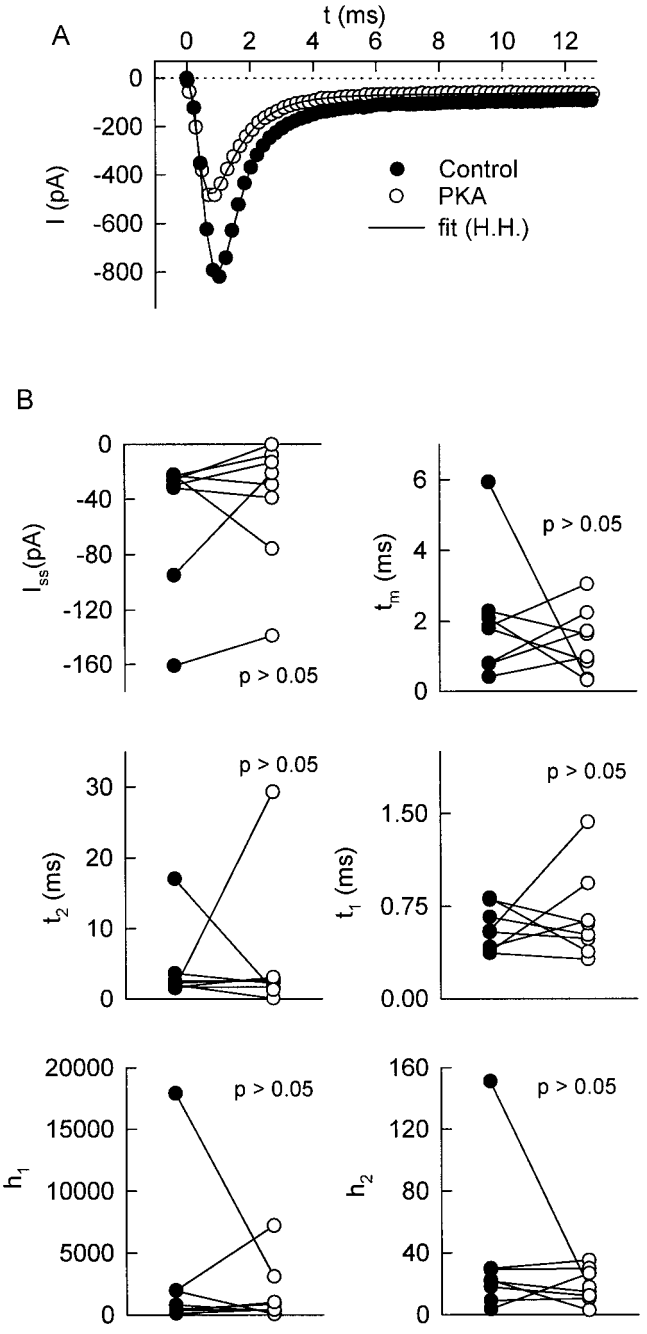

FIGURE 10 Analysis of experimental traces obtained at the beginning (●) or the end (○) of recordings of PKA catalytic unit loaded neurons, using the Hodgkin and Huxley model (Eq. 10). (*A*) Typical experimental traces (out of six pairs) showing PKA-induced current reduction. Holding potential = −80 mV; test pulse potential = −20 mV. (*B*) Effect of PKA-induced phosphorylation on the kinetic parameters. Scatter plots of I_{ss}, t_m, t_1, t_2, h_1, and h_2 values for six individual neurons. No parameter exhibits any significant change due to the addition of PKA catalytic unit treatment.

from the fact that the mean lag before channel opening is now increased by phosphorylation, but the mean open time remains unchanged. Thus, the mean net charge movement during an opening is also unchanged, though delayed, leading to a shift of the current trace to the right. This characteristic is clearly not compatible with the experimentally observed curves, suggesting that the phosphorylation-induced inhibition of the Na^+ current cannot be explained by a decreased rate of channel activation.

Interestingly, if phosphorylation accelerates the inactivation from the open state, then the mean open time is de-

creased, as well as the mean net charge movement, contrary to the case in which the inhibition is due to a decreased rate of activation. The fact that the channel inhibition obeys one or another mechanism is not without physiological consequence, as shown in Fig. 9 *C*: for a same decrease of the peak amplitude, the cumulated amount of net charge going into the cell is drastically different depending on whether the inhibition is due to a decrease of k_{CO} or an increase of k_{OI1}. In the former case, the effect of the inhibition simply delays the rise of charge. In the latter case, corresponding to the actual situation, the net amount of charge passing through the channels markedly falls down at any time. These mechanisms would therefore result in subtle but important differences in the regulation of action-potential generation, duration, and frequency.

Two previous studies proposed, on the basis of fragmentary data, that the phosphorylation-induced inhibition of the Na^+ channel does not involve any alteration of the mechanism of channel inactivation: on one hand, the inhibition apparently persisted in the presence of the batrachotoxin, which was known to block the inactivation process (Cukierman, 1996), and, on the other hand, the inhibition by phosphorylation was reported with a channel variant which did not exhibit inactivation (Smith and Goldin, 1997). In an attempt to reconcile our results with these observations, we could tentatively infer that, because the phosphorylation site recognized by the kinase A is situated in the I–II linker of the brain channel, different from the III–IV linker responsible for the classical channel inactivation, phosphorylation would induce the formation of an inactivated state different from the one which may be blocked either by the batrachotoxin or by the specific mutation. The proposed kinetic analysis developed in this study is certainly not capable of detecting the existence of a new inactivated state different from the classically described state. The observed increase of k_{OI1} would simply reflect the acceleration of the global inactivation process.

Na^+ channel has been demonstrated to be a substrate for PKC. The effects of phosphorylation by PKC are known to be different from those elicited by PKA because the voltage-dependence of the steady-state inactivation or the kinetics of the time-dependent inactivation were affected by PKC (Dascal and Lotan, 1991; Numann et al., 1991; West et al., 1991; Godoy and Cukierman, 1994a,b; O'Reilly et al., 1997). Godoy and Cukierman (1994a) have proposed that the PKC-induced phosphorylation of the channel accelerates the inactivation from the closed state. Our results suggest that this mechanism is not relevant in what concerns the effect of PKA phosphorylation. Indeed, after a conditioning potential pulse, the number of channels still susceptible to respond to depolarization appeared to be the same in the absence or in the presence of a phosphorylating treatment.

In brain, several neurotransmitters would be able to affect the activity of Na^+ channels through a PKA-induced phosphorylation, which would lead to the presented proposed alteration in Na^+ channel gating mechanism.

The authors would like to thank Dr. J. E. Dumont and Dr. J. J. Vanderhaeghen for their support in this work. This study was supported by the Belgian Program on University Poles of Attraction (initiated by the Belgian State, Prime Minister's office, Service for Sciences, Technology and Culture) and the Queen Elisabeth Medical Foundation (FMRE-Neurobiology 96–98), the Fund for Medical Scientific Research (FRSM-Belgium) and the European Biomed 2 project (BM4-CT96-0238). We are grateful to Roberte Menu and Michele Authelet for the expert technical assistance.

REFERENCES

Aldrich, R. W., D. P. Corey, and C. F. Stevens. 1983. A reinterpretation of mammalian sodium channel gating based on single channel recording. *Nature*. 306:436–441.

Aldrich, R. W., and C. F. Stevens. 1983. Inactivation of open and closed sodium channels determined separately. *Cold Spring Harb. Symp. Quant. Biol.* 48:147–153.

Armstrong, C. M. 1981. Sodium channels and gating currents. *Physiol. Rev.* 61:644–683.

Bean, B. P. 1981. Sodium channel inactivation in the crayfish giant axon. Must channels open before inactivating? *Biophys. J.* 35:595–614.

Cantrell, A. R., R. D. Smith, A. L. Goldin, T. Scheuer, and W. A. Catterall. 1997. Dopaminergic modulation of sodium current in hippocampal neurons via cAMP-dependent phosphorylation of specific sites in the sodium channel α subunit. *J. Neurosci.* 17:7330–7338.

Catterall, W. A. 1992. Cellular and molecular biology of voltage-gated sodium channels. *Physiol. Rev.* 72:S15–S48

Costa, M. R., J. E. Casnellie, and W. A. Catterall. 1982. Selective phosphorylation of the alpha subunit of the sodium channel by cAMP-dependent protein kinase. *J. Biol. Chem.* 257:7918–7921.

Costa, M. R., and W. A. Catterall. 1984. Cyclic AMP-dependent phosphorylation of the alpha subunit of the sodium channel in synaptic nerve ending particles. *J. Biol. Chem.* 259:8210–8218.

Cukierman, S. 1996. Regulation of voltage-dependent sodium channels. *J. Membr. Biol.* 151:203–214.

Dascal, N., and I. Lotan. 1991. Activation of protein kinase C alters voltage dependence of a Na^+ channel. *Neuron*. 6:165–175.

Fraser, D. D., K. Hoehn, S. Weiss, and B. A. MacVicar. 1993. Arachidonic acid inhibits sodium currents and synaptic transmission in cultured striatal neurons. *Neuron*. 11:633–644.

Gershon, E., L. Weigl, I. Lotan, W. Schreibmayer, and N. Dascal. 1992. Protein kinase A reduces voltage-dependent Na+ current in *Xenopus* oocytes. *J. Neurosci.* 12:3743–3752.

Godoy, C. M., and S. Cukierman. 1994a. Diacylglycerol-induced activation of protein kinase C attenuates Na^+ currents by enhancing inactivation from the closed state. *Pflugers Arch.* 429:245–252.

Godoy, C. M., and S. Cukierman. 1994b. Multiple effects of protein kinase C activators on Na^+ currents in mouse neuroblastoma cells. *J. Membrane Biol.* 140:101–110.

Goldman, L. 1995. Sodium channel inactivation from closed states: evidence for an intrinsic voltage dependency. *Biophys. J.* 69:2369–2377.

Hamill, O. P., A. Marty, E. Neher, B. Sakmann, and F. J. Sigworth. 1981. Improved patch-clamp techniques for high-resolution current recording from cells and cell-free membrane patches. *Pflugers Arch.* 391:85–100.

Hebert, T. E., R. Monette, J. C. Stone, P. Drapeau, and R. J. Dunn. 1994. Insertion mutations of the RIIA Na+ channel reveal novel features of voltage gating and protein kinase A modulation. *Pflugers Arch.* 427: 500–509.

Hille, B. 1992. Ionic Channels of Excitable Membranes. Sinauer Associates Inc., Sunderland, MA.

Hirschberg, B., A. Rovner, M. Lieberman, and J. Patlak. 1995. Transfer of twelve charges is needed to open skeletal muscle Na^+ channels. *J. Gen. Physiol.* 106:1053–1068.

Hodgkin, A. L., and Huxley, A. F. 1952. A quantitative description of membrane current and its application to conduction and excitation in nerve. *J. Physiol.* 117:500–544.

Horn, R., J. Patlak, and C. F. Stevens. 1981. Sodium channels need not open before they inactivate. *Nature*. 291:426–427.

Horn, R., and C. A. Vandenberg. 1984. Statistical properties of single sodium channels. *J. Gen. Physiol.* 84:505–534.

Lauger, P., W. Stephan, and E. Frehland. 1980. Fluctuations of barrier structure in ionic channels. *Biochim. Biophys. Acta*. 602:167–180.

Li, M., J. W. West, Y. Lai, T. Scheuer, and W. A. Catterall. 1992. Functional modulation of brain sodium channels by cAMP-dependent phosphorylation. *Neuron*. 8:1151–1159.

Li, M., J. W. West, R. Numann, B. J. Murphy, T. Scheuer, and W. A. Catterall. 1993. Convergent regulation of sodium channels by protein kinase C and cAMP-dependent protein kinase. *Science*. 261:1439–1442.

Marban, E., T. Yamagishi, and G. F. Tomaselli. 1998. Structure and function of voltage-gated sodium channels. *J. Physiol. Lond.* 508: 647–657.

McPhee, J. C., D. S. Ragsdale, T. Scheuer, W. A. Catterall. 1995. A critical role for transmembrane segment IVS6 of the sodium channel α subunit in fast inactivation. *J. Biol. Chem.* 270:12025–12034.

Murphy, B. J., S. Rossie, J. K. De, and W. A. Catterall. 1993. Identification of the sites of selective phosphorylation and dephosphorylation of the rat brain Na+ channel alpha subunit by cAMP-dependent protein kinase and phosphoprotein phosphatases. *J. Biol. Chem.* 268:27355–27362.

Nicoll, R. A., R. C. Malenka, and J. A. Kauer. 1990. Functional comparison of neurotransmitter receptor subtypes in mammalian central nervous system. *Physiol. Rev.* 70:513–565.

Numann, R., W. A. Catterall, and T. Scheuer. 1991. Functional modulation of brain sodium channels by protein kinase C phosphorylation. *Science*. 254:115–118.

O'Reilly, J. P., T. R. Cummins, and G. G. Haddad. 1997. Oxygen deprivation inhibits Na^+ current in rat hippocampal neurones via protein kinase C. *J. Physiol. Lond.* 503:479–488.

Patlak, J. 1991. Molecular kinetics of voltage-dependent Na^+ channels. *Physiol. Rev.* 71:1047–1080.

Rossie, S., and W. A. Catterall. 1987. Cyclic-AMP-dependent phosphorylation of voltage-sensitive sodium channels in primary cultures of rat brain neurons. *J. Biol. Chem.* 262:12735–12744.

Sarkar, S. N., A. Adhikari, and S. K. Sikdar. 1995. Kinetic characterization of rat brain type IIA sodium channel alpha-subunit stably expressed in a somatic cell line. *J. Physiol. Lond.* 488:633–645.

Schiffmann, S. N., P. M. Lledo, and J. D. Vincent. 1995. Dopamine D1 receptor modulates the voltage-gated sodium current in rat striatal neurones through a protein kinase A. *J. Physiol. Lond.* 483:95–107.

Schiffmann, S. N., F. Desdouits, R. Menu, P. Greengard, J.-D. Vincent, J.-J. Vanderheagen, and J.-A. Girault. 1998. Modulation of the voltage-gated sodium current in rat striatal neurons by DARPP-32, an inhibitor of protein phosphatase. *Eur. J. Neurosci.* 10:1312–1320.

Sigg, D., and F. Bezanilla. 1997. Total charge movement per channel. The relation between gating charge displacement and the voltage sensitivity of activation. *J. Gen. Physiol.* 109:27–39.

Sigworth, F. J. 1995. Charge movement in the sodium channel. *J. Gen. Physiol.* 106:1047–1051.

Smith, R. D., and A. L. Goldin. 1992. Protein kinase A phosphorylation enhances sodium channel currents in *Xenopus* oocytes. *Am. J. Physiol.* 263:C660–C666

Smith, R. D., and A. L. Goldin. 1997. Phosphorylation at a single site in the rat brain sodium channel is necessary and sufficient for current reduction by protein kinase A. *J. Neurosci.* 17:6086–6093.

Stevens, C. F. 1978. Interactions between intrinsic membrane protein and electric field. An approach to studying nerve excitability. *Biophys. J.* 22:295–306.

Stimers, J. R., F. Bezanilla, and R. E. Taylor. 1985. Sodium channel activation in the squid giant axon. Steady state properties. *J. Gen. Physiol.* 85:65–82.

Surmeier, D. J., J. Eberwine, C. J. Wilson, Y. Cao, A. Stefani, and S. T. Kitai. 1992. Dopamine receptor subtypes colocalize in rat striatonigral neurons. *Proc. Natl. Acad. Sci. USA*. 89:10178–10182.

Vandenberg, C. A., and R. Horn. 1984. Inactivation viewed through single sodium channels. *J. Gen. Physiol.* 84:535–564.

Vandenberg, C. A., and F. Bezanilla. 1991. A sodium channel gating model based on single channel, macroscopic ionic, and gating currents in the squid giant axon. *Biophys. J.* 60:1511–1533.

West, J. W., R. Numann, B. J. Murphy, T. Scheuer, and W. A. Catterall. 1991. A phosphorylation site in the Na^+ channel required for modulation by protein kinase C. *Science*. 254:866–868.

Zhang, X. F., X. T. Hu, and F. J. White. 1998. Whole-cell plasticity in cocaine withdrawal: reduced sodium currents in nucleus accumbens neurons. *J. Neurosci.* 18:488–498.